Object-Oriented Software Development and High-Performance Technologies for Identifying Complex Processes in Nanoporous System

Mykhaylo Petryk[1, †], Igor Boyko[1,*†] and Anatolii Doroshenko[2,†]

[1] *Ternopil Ivan Puluj National Technical University, Rus'ka St, 56, Ternopil, 46001, Ukraine*
[2] *National Technical University of Ukraine "Igor Sikorsky Kiev Polytechnic Institute", Peremohy Ave, 37, Kyiv, 03056, Ukraine*

Abstract

Advanced high-performance supercomputer technologies have been developed for detailed modeling and precise identification of key parameters in complex multicomponent competitive adsorption processes within nanoporous systems with feedback. A unique feature is the presence of feedback-driven processes, making their dynamics especially relevant for scientific study. These technologies use powerful mathematical tools, including the Laplace transform for analyzing dynamic systems and the Heaviside operational method for solving complex differential equations. Such methods are well-suited for modeling systems with feedback, ensuring accurate and stable simulations. Special focus is placed on decomposing nonlinear functions describing competitive adsorption equilibrium, particularly Langmuir isotherm-based models for gas adsorption on solid surfaces. The approach includes efficient parallelization of model vector components, significantly accelerating computations for multidimensional problems by utilizing multi-core processors. This allows reduced simulation times and processing of larger, more complex systems. The paper presents the results of extensive numerical experiments conducted using high-speed parallel computing on modern multi-core architectures. The outcomes demonstrate the efficiency and accuracy of the developed technologies for modeling and identifying parameters that govern complex adsorption behavior. The results significantly impact the advancement of materials and emerging technologies in domains like catalysis, gas separation, and energy storage, where accurate prediction of adsorption is vital for optimizing and designing sustainable systems.

Keywords

competitive adsorption, Langmuir equilibrium, parallel computing, Heaviside operational method

1. Introduction

The application of cutting-edge artificial intelligence technologies and cyber-physical systems to the regulation of toxic gas release into the atmosphere offers promising potential for improving environmental conditions and human health, building safe energy and transport infrastructures, and introducing effective strategies to mitigate the impacts of global temperature rise[1]. The quality of mathematical models describing complex processes of competitive adsorption of multiple gases in nanoporous cyber-systems—while accounting for feedback from nanophysical factors that limit internal kinetics during these processes—and the efficiency of high-performance computational methods for solving such models using modern computing technologies determine the effectiveness of addressing these challenges [2]. Currently, several theoretical and experimental studies are being conducted on the development of such cyber-physical systems, which are

Workshop "Intelligent information technologies" UkrProg-IIT`2025 co-located with 15th International Scientific and Practical Programming Conference UkrPROG'2025", May 13-14, 2025, Kyiv, Ukraine
[1*] Corresponding author.
[†] These authors contributed equally.
petrykmr@gmail.com (M. Petryk); boyko.i.v.theory@gmail.com (I. Boyko); doroshenkoanatoliy2@gmail.com (A. Doroshenko)
0000-0001-6612-7213 (M. Petryk); 0000-0003-2787-1845 (I. Boyko); 0000-0002-8435-1451 (A. Doroshenko)

fundamentally based on mathematical models of complex competitive gas adsorption processes, incorporating various internal kinetic limitations in nanoporous environments [2–7]. However, existing models do not fully represent the comprehensive nature of internal kinetics in nanoprocesses of multicomponent competitive adsorption. They often fail to account for a broad spectrum of key influencing factors and feedback mechanisms that govern interactions between components, including the conditions of competitive adsorption equilibrium and the mutual influence of adsorbed species on both macro- and microscales.

A noticeable gap exists in the availability of precise mathematical modeling that fully incorporate such limiting physical feedbacks in competitive nano-adsorption, which hinders a complete understanding of transport phenomena, as well as the development of high-performance computational methods for their implementation. In this work, continuing the studies presented in [4, 8–12], we justify and develop high-performance mathematical modeling methods for competitive adsorption and "competitive diffusion" of multiple gases in nanoporous cyber-systems. The approach is based on a generalized nonlinear Langmuir competitive isotherm, which most comprehensively reflects feedback mechanisms and adsorption equilibrium on nanopore surfaces.

To model these processes, we apply advanced methods, including the Laplace integral transform, Heaviside operational calculus, and a decomposition-based approach for complex models of nanoporous cyber-systems involving n interrelated nonlinear adsorption equilibrium equations. This framework enables the derivation of high-speed analytical solutions, improving the efficiency of computational parallelization and the accuracy of modeling and identification on multi-core computing platforms.

2. Development of the mathematical model of competitive adsorption of multiple gases grounded in a modified Langmuir framework describing equilibrium under competitive adsorption conditions

The influx of a multicomponent gas mixture undergoes diffusion both through the macropores (interparticle voids) of the nanoporous system and within the nanopores of the individual particles. The core hypothesis of the developed framework assumes the presence of interactive adsorption effects between components, which are governed by the conditions of competitive adsorption equilibrium between the adsorbate molecules and active adsorption sites on the phase interfaces within the nanopores. The general assumption underlying the proposed model is that mutual adsorption interactions between different gas molecules (two or more) and active sites on the phase boundaries of nanoporous particles are described by a vector function of nonlinear Langmuir-type adsorption equilibrium. This formulation accounts for the mutual influence of all adsorbate components under the defined physical conditions [7]. The developed model, structurally based on a bipore concept [2, 3, 5, 6], follows the methodological approach introduced by Ruthven and Karger [7, 8], as demonstrated in the studies by Petryk and Fraissard [9]. It captures the complex phenomena of competitive adsorption and co-diffusion, relying on the following key assumptions:

1. Competitive adsorption of multiple gases arises from dispersion and electrostatic (Johns-Lenard) forces. It includes intermolecular competition among various adsorbate species, as well as competitive diffusion in the macropores (interparticle space) and micropores of spherical particles (intraparticle space). All nanoporous particles (crystallites) are assumed to have an identical radius R and are uniformly packed in the catalyst's active region.

2. Competitive adsorption and diffusion take place at active sites located on the internal surfaces of the nanoporous medium [7, 8]. These active centers adsorb different components of the mixture in unequal proportions, forming multilayer molecular films on their surfaces. As the system evolves toward equilibrium, concentration gradients of individual adsorbate species develop in both macro- and micropores.

3. The dynamics of this process depend on the qualitative and quantitative composition of the diffusing adsorbate flux. Asymmetric interaction effects - studied separately for two-component

systems by Petryk, Fraissard, and Deyneka [7, 8] - emerge due to the distinct adsorption and diffusion behavior of two adsorbate species in the micropores of the catalyst. For example, the presence of component *j* alters the diffusion of component *i*, and vice versa, when $i \neq j$. Theoretical and experimental studies have demonstrated this asymmetry in systems like "benzene in the presence of hexane" and "hexane in the presence of benzene," in equimolar mixtures using nanoporous zeolite catalysts [7, 8].

Finally, the kinetics of competitive adsorption of n gas components ($n \geq 2$) in nanoporous cyber-physical systems designed for the capture of gas emissions, incorporating the nonlinear adsorption equilibrium function and the aforementioned physical assumptions, is governed by the following system of nonlinear partial differential equations [13–15]:

$$\frac{\partial C_j(t,Z)}{\partial t} = \frac{D_{inter_j}}{l^2}\frac{\partial^2 C_j}{\partial Z^2} - e_{inter_j}\frac{D_{intra_j}}{R^2}\left(\frac{\partial Q_j}{\partial X}\right)_{X=1} \tag{1}$$

$$\frac{\partial Q_j(t,X,Z)}{\partial t} = \frac{D_{intra_j}}{R^2}\left(\frac{\partial^2 Q_j}{\partial X^2} + \frac{2}{X}\frac{\partial Q_j}{\partial X}\right) \tag{2}$$

with initial conditions

$$C_j(t=0,Z)=0;\ Q_j(t,X,Z)_{|t=0}=0;\ X\in(0,1),\ j=\overline{1,n}, \tag{3}$$

boundary conditions along the X coordinate – radius of the particle:

$$\frac{\partial Q_j(t,X,Z)_{|X=0}}{\partial X}=0, \tag{4}$$

- conditions of Langmuir competitive-adsorption equilibrium at the boundary X=1:

$$Q_j(t,X=1,Z)_{|X=1} = \frac{K_j C_j(t,Z)}{1+K_1C_1(t,Z)+K_2C_2(t,Z)+\ldots+K_nC_n(t,Z)},\quad j=\overline{1,n} \tag{5}$$

boundary conditions along the Z coordinate:

$$C_j(t,Z)_{|Z=1}=C_j^{in};\ \frac{\partial}{\partial Z}C_j(t,Z)_{|Z=0}=0. \tag{6}$$

Here c_j, q_j, - current concentrations of diffused adsorbent components in the interparticle space (interparticle space) and micropores of particles (intraparticle space), $c_{\infty j}$, $q_{\infty j}$,- the corresponding equilibrium concentrations of the adsorbent components of the gas and adsorbed phases, *n* - the total number of diffused adsorbent components, $\text{К}_j^0 = q_{\infty_j}/c_{\infty_j}$ - the adsorption constant of the *jth* adsorbent component, $K_j = 1/\text{К}_j^0,\ j=\overline{1,n}$, $\varepsilon_{\text{inter}}$ - the macroporosity of the medium, $e_{\text{inter}_j} = \varepsilon_{\text{inter}}c_j/(\varepsilon_{\text{inter}}c_j+(1-\varepsilon_{\text{inter}})q_j) \approx \varepsilon_{\text{inter}}/(1-\varepsilon_{\text{inter}})\text{К}_j^0$, $e_{\text{intra}_j} = 1-e_{\text{inter}_j}$, $j=\overline{1,n}$.

Decomposition of the nonlinear system (1)-(6) were performed on basis of nonlinear function of the multicomponent competitive Langmuir adsorption equilibrium

$$\varphi_j(C_1,C_2,\ldots,C_n) = K_jC_j(t,Z)/\left[1+\sum_{j_1=1}^{n}K_{j_1}C_{j_1}(t,Z)\right],\quad j=\overline{1,n}. \tag{7}$$

we expand in a Maclaurin series in the vicinity of the point of zero concentrations of the diffused adsorbate components [7]. For simplicity of the decomposition and further calculations, only three components will be considered in the present study (n =3):

$$\varphi_i^0(C_1,C_2,C_2) = \varphi_i^0 + \left(\frac{\partial\varphi_i^0}{\partial C_1}C_1+\frac{\partial\varphi_i^0}{\partial C_2}C_2+\frac{\partial\varphi_i^0}{\partial C_3}C_3\right)+\frac{1}{2}\left(\frac{\partial^2\varphi_i^0}{\partial C_1^2}C_1^2+\frac{\partial^2\varphi_i^0}{\partial C_2^2}C_2^2+\frac{\partial^2\varphi_i^0}{\partial C_3^2}C_3^2\right)+$$
$$+\left(\frac{\partial^2\varphi_i^0}{\partial C_1\partial C_2}C_1C_2+\frac{\partial^2\varphi_i^0}{\partial C_1\partial C_3}C_1C_3+\frac{\partial^2\varphi_i^0}{\partial C_2\partial C_3}C_2C_3\right)+\ldots \tag{8}$$

where $\varphi_i^0 = \varphi_i\left(0,0,0\right)$.

As a result, for equations (8) we obtain the following second-order expansions of accuracy

$$Q_1\left(t,X=1,Z\right)_{|X=1} = K_1\left(\mathrm{C}_1 - K_1C_1^2 - K_2C_1C_2 - K_3C_1C_3\right);$$
$$Q_2\left(t,X=1,Z\right)_{|X=1} = K_2\left(\mathrm{C}_2 - K_2C_2^2 - K_1C_1C_2 - K_3C_2C_3\right);$$
$$Q_3\left(t,X=1,Z\right)_{|X=1} = K_3\left(\mathrm{C}_3 - K_3C_3^2 - K_1C_1C_3 - K_2C_2C_3\right), \quad (9)$$

Assuming that $K_1 = \max\left\{K_j,\ K_j<1\right\}_{j=1}^{n}$ is a small parameter ($\varepsilon = K_1^2 << 1$), the boundary value problem defined by equations (1)–(6), together with the approximate kinetic phase transformation equation (9), which also involves this small parameter, can be treated as a mixed-type boundary problem for a nonlinear system of partial differential equations. To solve this system, we apply the method of asymptotic expansions in powers of the small parameter, representing the solution as a formal power series, as suggested in [10]:

$$C_j\left(t,\mathrm{Z}\right) = C_{j_0}\left(t,\mathrm{Z}\right) + \varepsilon C_{j_1}\left(t,\mathrm{Z}\right) + \varepsilon^2 C_{j_2}\left(t,\mathrm{Z}\right) + \ldots, \quad (10)$$

$$Q_j\left(t,X,Z\right) = Q_{j_0}\left(t,X,Z\right) + \varepsilon Q_{j_1}\left(t,X,Z\right) + \varepsilon^2 Q_{j_2}\left(t,X,Z\right) + \ldots,\ j=\overline{1,3}. \quad (11)$$

By substituting the asymptotic expansions (10) and (11) into equations (1)–(6), and applying the transformation $N_j = XQ_j$, the original nonlinear boundary value problem (1)–(6) is decomposed into two categories of linearized boundary value problems [10]:

Problem $A_{j_0},\ j=\overline{1,n}$: find $D=\left\{\left(t,\mathrm{X},\mathrm{Z}\right):\ t>0,\ \ X\in\left(0,1\right),Z\in\left(0,1\right)\right\}$ the solution to the system of partial differential equations in the domain :

$$\frac{\partial}{\partial t}C_{j_0}\left(t,Z\right) = \frac{D_{inter_j}}{l^2}\frac{\partial^2 C_{j_0}}{\partial Z^2} - e_{inter_j}\frac{D_{intra_j}}{R^2}\left(\frac{\partial N_{j_0}}{\partial X} - N_{j_0}\right)_{X=1}, \quad (12)$$

$$\frac{\partial}{\partial t}N_{j_0}\left(t,X,Z\right) = \frac{D_{intra_j}}{R^2}\frac{\partial^2 N_{j_0}}{\partial X^2}, \quad (13)$$

with initial conditions:

$$C_{j_0}\left(t,Z\right)_{|t=0} = 0;\ N_{j_0}\left(t,X,Z\right)_{|t=0} = 0;\ X\in\left(0,1\right),\ j=\overline{1,n}, \quad (14)$$

boundary conditions along the X coordinate for a nanoporous particle:

$$N_{j_0}\left(t,X,Z\right)_{|X=0} = 0;\ N_{j_0}\left(t,X,Z\right)_{|X=1} = K_jC_{j_0}\left(t,Z\right),\quad j=\overline{1,n}, \quad (15)$$

boundary conditions along the Z coordinate :

$$C_{j_0}\left(t,Z\right)_{|Z=1} = 1;\ \ \frac{\partial}{\partial Z}C_{j_0}\left(t,Z\right)_{|Z=0} = 0, \quad (16)$$

Problem $A_m,\ m=\overline{1,\infty}$: to construct a bounded solution is associated with the system of equations in the domain D

$$\frac{\partial C_{j_m}}{\partial t}\left(t,Z\right) = \frac{D_{inter_j}}{l^2}\frac{\partial^2 C_{j_m}}{\partial Z^2} - e_{\mathrm{inter}_j}\frac{D_{intra_j}}{R^2}\left(\frac{\partial N_{j_m}}{\partial X} - N_{j_m}\right)_{X=1}, \quad (17)$$

$$\frac{\partial}{\partial t}N_{j_m}\left(t,X,Z\right) = \frac{D_{intra_j}}{R^2}\frac{\partial^2 N_{j_m}}{\partial X^2} \quad (18)$$

assuming zero initial conditions:

$$C_{j_m}\left(t,Z\right)_{|t=0} = 0;\ N_{j_m}\left(t,X,Z\right)_{|t=0} = 0;\ j=\overline{1,n}, \quad (19)$$

boundary conditions along the X coordinate for the particle:

$$N_{j_m}\left(t,X,Z\right)_{|X=0}=0;\ N_{j_m}\left(t,X,Z\right)_{X=1}=K_jC_{j_m}\left(t,Z\right)-F_{j_m}\left(t,Z\right),\ \ j=\overline{1,n}$$

$$F_{j_m}\left(t,\mathrm{Z}\right)=\sum_{s=0}^{m-1}\sum_{k=1}^{n}\frac{K_jK_k}{K_1^2}C_{j_s}\left(t,\mathrm{Z}\right)C_{k_{m-1-s}}\left(t,\mathrm{Z}\right),\ \ j=\overline{1,n}\quad,\qquad(20),$$

boundary conditions along the Z coordinate:

$$C_{j_m}\left(t,Z\right)_{|Z=1}=0;\ \frac{\partial}{\partial Z}C_{j_m}\left(t,Z\right)_{|Z=0}=0\quad.\qquad(21)$$

In the final form, the solutions of problem (12)-(21) are given by as follows:

$$C_{j_m}(t,X,Z)=-\frac{3}{e_{\mathrm{inter}_j}}\frac{l^2}{\mathrm{R}^2}\frac{\mathrm{D}_{\mathrm{intra}_j}}{\mathrm{D}_{\mathrm{inter}_j}}\int_0^t\left(\begin{array}{l}\int_Z^1\left(\mathrm{H}_j^-\left(t-\tau,Z,\xi\right)-\mathrm{K}_j^-\left(t-\tau,Z,\xi\right)\right)F_{j_m}\left(\tau,\xi\right)d\xi+\\+\int_0^Z\left(\mathrm{H}_j^+\left(t-\tau,Z,\xi\right)-\mathrm{K}_j^+\left(t-\tau,Z,\xi\right)\right)F_{j_m}\left(\tau,\xi\right)d\xi\end{array}\right)d\tau,\ \ j=\overline{1,n}\quad,\qquad(22)$$

$$Q_{j_m}\left(t,X,Z\right)=\int_0^t\left(K_jC_{j_m}\left(t-\tau,Z\right)-\sum_{s=0}^{m-1}\sum_{k=1}^{3}\frac{K_jK_k}{K_1^2}C_{j_s}\left(t-\tau,\mathrm{Z}\right)C_{k_{m-1-s}}\left(t-\tau,\mathrm{Z}\right)\right)\times$$

$$\times\left(2\frac{\mathrm{D}_{\mathrm{intra}_j}}{\mathrm{R}^2}\sum_{k_2=0}^{\infty}\frac{\pi k_2\cdot\sin\left(k_2\pi X\right)()}{\left(-1\right)^{k_2+1}X}\exp\left(-\frac{\mathrm{D}_{\mathrm{intra}_j}}{\mathrm{R}^2}{k_2}^2\pi^2t\right)\right)d\tau,\ \ j=\overline{1,3}\quad.\qquad(23)$$

where $\mathrm{H}_j^-\left(t-\tau,Z,\xi\right),\ \mathrm{K}_j^-\left(t-\tau,Z,\xi\right),\ \mathrm{H}_j^+\left(t-\tau,Z,\xi\right),\ \mathrm{K}_j^+\left(t-\tau,Z,\xi\right)$ - components of the Cauchy influence function the algorithm for calculating which is given below, $p_{k_2}^j=-\pi^2{k_2}^2D_{\mathrm{intra}_j}/R^2,\ k_2=\overline{0,\infty}$ - roots of the equation;

$$\mathrm{sh}\left(R\sqrt{\frac{p}{\mathrm{D}_{\mathrm{intra}_j}}}\right)=0\quad.\qquad(24)$$

Calculation of the original components of the influence functions were performed as follows. Applying $\mathrm{H}_j\left(t,Z,\xi\right)$ Heaviside's theorem to the components of the influence functions, we obtain:

$$L^{-1}\left[\frac{f_j^h\left(p\right)}{\gamma_j\left(p\right)sh\left[\gamma_j(p)\right]\mathrm{c}\,h\left[\gamma_j(p)\right]}\right]=$$

$$=\sum_{s=1}^{\infty}\sum_{k=1}^{\infty}\frac{f_j^h\left(\beta_{ks}^j\right)e^{\frac{\mathrm{D}_{\mathrm{intra}_j}}{R^2}\left(\beta_{ks}^j\right)^2t}}{\omega_j^1\left(\beta_{ks}^j\right)}+\sum_{s_1=1}^{\infty}\frac{f_j^h\left(\mu_{s_1}^j\right)e^{\frac{\mathrm{D}_{\mathrm{intra}_j}}{R^2}\left(\mu_{s_1}^j\right)^2t}}{\nu_j^2\left(\mu_{s_1}^j\right)}+\sum_{k_1=1}^{\infty}\frac{f_j^h\left(\eta_{k_1}^j\right)e^{\frac{\mathrm{D}_{\mathrm{intra}_j}}{R^2}\left(\eta_{k_1}^j\right)^2t}}{\omega_j^2\left(\eta_{k_1}^j\right)}\qquad(25)$$

We calculate the denominators in the expressions of the sums of each component of the right-hand side of formula (24):

$$\omega_j^1\left(\beta_{ks}^j\right)\equiv\gamma_j\left(p\right)sh\left(R\sqrt{\frac{p}{\mathrm{D}_{\mathrm{intra}_j}}}\right)\frac{d}{dp}\mathrm{c}\,h\left[\gamma_j(p)\right]\Big|_{p=\beta_{ks}^j}=$$

$$=-\gamma_j\left(\beta_{ks}^j\right)\sin\left(\beta_{ks}^j\right)\frac{\left(-1\right)^k\beta_{ks}^{j2}}{2k-1}\left[\frac{3K_j}{\mathrm{e}_{\mathrm{inter}_j}}\left(\frac{1}{\sin^2(\beta_{ks}^j)}-\frac{ctg(\beta_{ks}^j)}{\beta_{ks}^j}\right)+2\right],\qquad(26)$$

where $\left\{\beta_{ks}^j\right\},k,s=\overline{1,\infty}$ is the set of positive roots of the transcendental equation (24) .

Next,

$$\nu_j^1\left(\mu_{s_1}^j\right)\equiv\gamma_j(p)\,ch\left[\gamma_j(p)\right]\frac{d}{dp}sh\left(R\sqrt{\frac{p}{\mathrm{D}_{\mathrm{intra}_j}}}\right)\Bigg|_{p=-\frac{\mathrm{D}_{\mathrm{intra}}}{R^2}\mu_{s_1}^{j\,2}}=$$

$$=\gamma_j\left(\mu_{s_1}^j\right)\cos\left[\gamma_j\left(\mu_{s_1}^j\right)\right](-1)^{s_1}\frac{R^2}{2\mathrm{D}_{\mathrm{intra}_j}\mu_{s_1}^j}\Bigg|_{\mu_{s_1}^j=\pi s_1};$$

$$\omega_j^2\left(\eta_{k_1}^j\right)=-\frac{l}{2R}\sqrt{\frac{3K_j}{e_{\mathrm{inter}_j}}\frac{\mathrm{D}_{\mathrm{intra}_j}}{\mathrm{D}_{\mathrm{inter}_j}}}\left(\frac{ctg\left(\eta_{k_1}^j\right)}{\eta_{k_1}^j}-\frac{1}{\sin^2\eta_{k_1}^j}+\frac{2e_{\mathrm{inter}_j}}{3}\right)\sin\left(\eta_{k_1}^j\right)\cos\left[\gamma_j\left(\eta_{k_1}^j\right)\right] \tag{27},$$

where $\left\{\eta_{k_2}^j\right\}_{k_2=\overline{1,\infty}}^{j=\overline{1,3}}$ - the set of positive roots of the equation:

$$\frac{e_{\mathrm{inter}_j}}{3K_j}\left(\mu^j\right)^2-\mu^j ctg\left(\mu^j\right)+1=0 \tag{28}.$$

As a result, we obtain the final expressions for the originals :

$$\mathrm{H}_j^-\left(t,Z,\xi\right)=\sum_{s=1}^{\infty}\sum_{k=1}^{\infty}\frac{\beta_{ks}^j\cos\left(\beta_{ks}^j\right)\sin\left(\gamma_j\left(\beta_{ks}^j\right)(1-\xi)\right)c\cos\left(\gamma_j\left(\beta_{ks}^j\right)Z\right)e^{\frac{\mathrm{D}_{\mathrm{intra}_j}}{R^2}\left(\beta_{ks}^j\right)^2t}}{\omega_j^1\left(\beta_{ks}^j\right)}+$$

$$\sum_{s_1=1}^{\infty}\frac{\mu_{s_1}^j\cos\left(\mu_{s_1}^j\right)\sin\left(\gamma_j\left(\mu_{s_1}^j\right)(1-\xi)\right)\cos\left(\gamma_j\left(\mu_{s_1}^j\right)Z\right)e^{\frac{\mathrm{D}_{\mathrm{intra}_j}}{R^2}\left(\mu_{s_1}^j\right)^2t}}{\nu_j^2\left(\mu_{s_1}^j\right)}+$$

$$+\sum_{k_1=1}^{\infty}\frac{\eta_{k_1}^j\cos\left(\eta_{k_1}^j\right)\sin\left(\gamma_j\left(\eta_{k_1}^j\right)(1-\xi)\right)\cdot\cos\left(\gamma_j\left(\eta_{k_1}^j\right)Z\right)e^{\frac{\mathrm{D}_{\mathrm{intra}_j}}{R^2}\left(\eta_{k_1}^j\right)^2t}}{\omega_j^2\left(\eta_{k_1}^j\right)}. \tag{29}$$

2. Software system architecture development and final modeling

The vector functions of dimension 2n×2M, obtained in results (20)-(29) of the competitive model, enable efficient parallelization of computations within the cyber-physical system. Here, denotes the maximum number of approximation elements in the nonlinear components of the solution. In real systems of competitive gas adsorption involving several dozen components, a significant performance gain is observed due to parallelization, where the parallel processing speed is proportional to 2n×2M compared to single-processor computations.

The developed parallel computation algorithms have been implemented in the form of software using Microsoft Visual Studio C++ 2019, utilizing the Parallel Patterns Library (PPL) [17] in accordance to general design automation methodology developed in [19].. This toolkit was employed to carry out system modeling. The general scheme of the parallelization algorithm based on the constructed vector solutions of model equations (1)–(6) is presented as a UML activity diagram in Fig. 1. To implement parallel computations based on the proposed mathematical model, computational templates of the concurrent sub vector PPL class were used, along with the algorithms concurrency: parallel_invoke and concurrency: parallel_for_each, with implementation elements provided in the program code below.

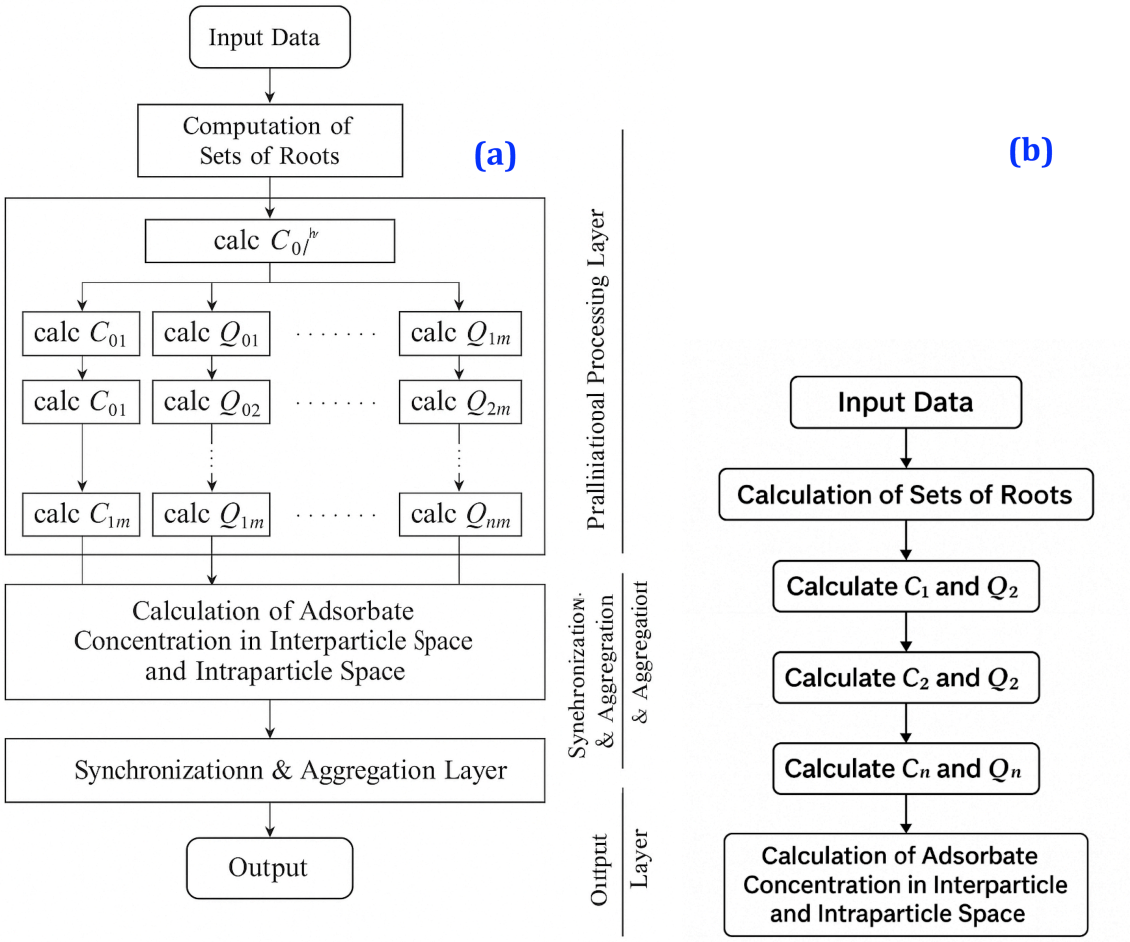

Figure 1: UML activity diagram (a) and architecture of the parallel algorithm (b).

Individual classes of headers and names of domain-specific objects are described as follows:
Macro_Pores_Concentration oC1, oC2; // distribution of concentrations of components
//(1,2) in interparticle space
Nano_Pores_Concentration oQ1, oQ2; // distribution of concentrations of components
//(1,2) in intraparticle space
Parallel data structures based on the concurrent_vector class from PPL, used in parallel computation algorithms:
concurrent_vector<Macro_Pores_Concentration>v_cZ;concurrent_vector<tuple<int,
concurrent_vector<Macro_Pores_Concentration_C>>>v_c_t_Z;
concurrent_vector<concurrent_vector<Macro_Pores_Concentration>>
mass_flow;concurrent_vector<Nano_Pores_Concentration> v_qZ;

A parallel computation block for the distribution of competitive adsorption concentrations (for component 1 in the interparticle space) in C++/PPL code (Microsoft VS 2019):

```
parallel_for_each (begin(a_t), end(a_t),
[&] (int n, float t){
parallel_for_each (begin(aZ), end(aZ),
[&] (float Z){oC1.Computing_C1(n,t,Z);
v_c_Z.push_back(oC1);});
v_c_t_Z.push_back(make_tuple(n, v_c_Z));});
```

A fragment of a parallel computation block for the distribution of competitive adsorption concentrations (for component 1 in the intraparticle space). To implement multi-level parallel calculations of competitive adsorption concentrations, the Microsoft Visual Studio C++ 2019 Parallel Patterns Library (PPL) was used. The parallel structure employs nested parallel_for_each

constructs, enabling the distribution of computations across multiple spatial dimensions. The following code snippet demonstrates the computation of component 1 concentration in the intraparticle space:

```
parallel_for_each(begin(a_t), end(a_t), [&] (int n, float t) {
parallel_for_each(begin(aZ), end(aZ), [&] (float Z) {
parallel_for_each(begin(aX), end(aX), [&] (float X) {
oQ1.Computing_Q1(n, t, Z, X);v_Q_X.push_back(oQ1);});
v_Q_Z.push_back(v_Q_X);});
v_c_t_Z.push_back(make_tuple(n, v_Q_Z));});
```

Here, the identifiers prefixed with calc1_, layer_, and elem_—referenced in both the diagram and code fragments—are utilized as method names, including overloaded versions, to support hierarchical parallelization.All computations were executed on a 64-core university-based high-performance computing cluster with shared memory. This allowed efficient resource utilization and significant performance improvements in solving the system model.

The adsorption process modeling for gas mixtures was carried out using standard geometric parameters of the adsorption column: L=0.3 m, R=0.1 m [2]. These values effectively define the boundary conditions $z=L$ and $x=R$. The physical properties of the gases applied in both direct calculations and simulations were sourced from references [2–4].

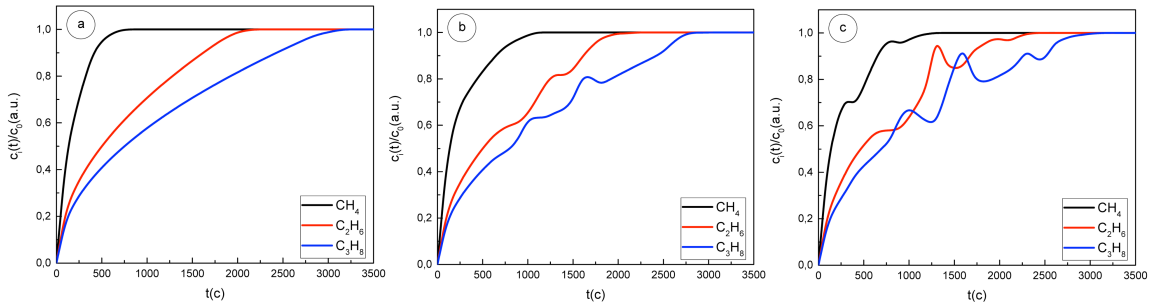

Figure 2: Breakthrough curves ($c_i(t)/c_0$, i =1,2,3) of adsorption for a mixture of methane (CH_4, i =1), ethane (C_2H_6, i =2), propane (C_3H_8, i =3) taken in different mass ratios in the input mixture: (80%, 15%, 5%) (a), (35%, 35%, 30%) (b), (10%, 45%, 45%) (c).

Fig. 2a, b, c illustrate the behavior of adsorption breakthrough curves computed for various mass fraction values of the components of methane, ethane and propane in the input mixture at room temperature (T =300K). At the same time, the first dependence calculated in Fig. 1a actually corresponds to the case of adsorption of natural gas, in which the distribution of components by mass fractions is approximately the same. As can be seen from the given dependencies, the adsorption curves for methane change little when the mass fractions of gases in the mixture change (Fig. 2a, b). Only with a significant decrease in the mass fraction of methane (Fig. 2c) does the dependence $c_1(t)/c_0$ partially deform, but adsorption reaches saturation at the same time point (t ~ 1300 c) as in the dependencies in Fig. 1a, b.

The adsorption of ethane and propane occurs in a completely different way. Despite the fact that in the case of small mass fractions of these gases, their adsorption occurs in a similar way to the adsorption of methane (Fig. 3a), with an increase in the mass fractions of ethane and propane, their adsorption reaches saturation in virtually the same time interval, the dependence $c_2(t)/c_0$ and $c_3(t)/c_0$ change significantly, forming additional maxima and minima and approaching each other. In this case, a case is possible when, in certain time intervals, the adsorption of propane is faster than for less volatile ethane molecules. This effect is due to the fact that in a stationary gas flow, during its laminar flow, the distribution of gas molecules in the mixture occurs according to the Maxwell-Boltzmann dependence, i.e. the actual concentrations of the components are proportional to the value: $\exp(-p^2/2kT)$, where m is the mass of the gas molecule, p is its

momentum, determined by the mean square velocity of motion. In our case, ethane and propane molecules, which have similar thermal motion energies, have the same statistical distribution, which leads to the collective effects shown in Fig. 3 b , c . For methane, such an effect is not observed, since its molecules are more volatile.

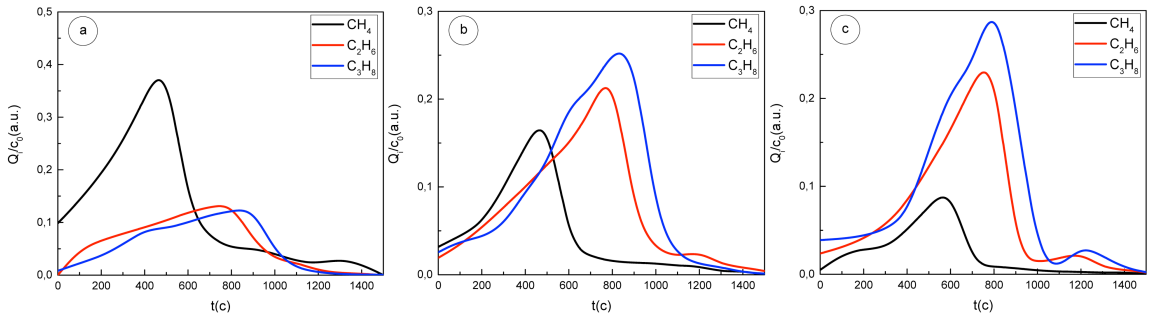

Figure 3: Desorption curves in zeolite nanopores ($Q_i(t)/c_0$, i =1,2,3) for a mixture of methane (CH_4 , i=1), ethane (C_2H_6 , i =2), propane (C_3H_8 , i =3) taken in different mass ratios in the input mixture: (80%, 15%, 5%) (*a*), (35%, 35%, 30%) (*b*), (10%, 45%, 45%) (*c*).

3. Conclusions

A novel approach based on high-performance parallel computing has been developed for the modeling and parameter identification of n-component competitive adsorption in nanoporous cybersystems, accounting for feedback interactions. An efficient strategy for the parallelization of the vector components of the solution was proposed through the decomposition of a nonlinear system incorporating Langmuir adsorption equilibrium conditions. The methodology applies Laplace integral transforms and the operational Heaviside method to enhance computational tractability.

Numerical simulations were carried out on multicore computing platforms utilizing high-speed parallel execution, resulting in substantial acceleration. The implementation of custom-designed parallel algorithms yielded a 10–15-fold increase in computational efficiency. For reference, a comparable non-parallelized computational approach requires approximately 3 to 5 hours of machine time to solve similar problems.

Declaration on Generative AI

The authors have not employed any Generative AI tools.

References

[1] N. Unger, T. C. Bond, J. S. Wang, D. M. Koch, S. Menon, D. T. Shindell, S. Bauer, Attribution of climate forcing to economic sectors, Proc. Natl. Acad. Sci. 107 (2010) 3382–3387. doi:10.1073/pnas.0906548107.

[2] B. Puertolas, M. V. Navarro, J. M. Lopez, R. Murillo, A. M. Mastral, T. Garcia. Modelling the heat and mass transfers of propane onto a ZSM-5 zeolite, Separation and Purification Technology, 86 (2012) 127–136. doi:10.1016/j.seppur.2011.10.011.

[3] A. Iliyas, H. M. Zahedi-Niaki, M. Eic. One-dimensional molecular sieves for hydrocarbon cold-start emission control: influence of water and CO_2, Appl. Catal. A, 382 (2010) 213–219. doi:10.1016/j.apcata.2010.04.040.

[4] J. Kärger, D. M. Ruthven, D. N. Theodorou. Diffusion in Nanoporous Materials. John Wiley & Sons, Hoboken, 2012. 660 p. doi:10.1002/9783527651276.

[5] I. Langmuir. The constitution and fundamental properties of solids and liquids. Part I. Solids, J. Am. Chem. Soc., 54 (1932) 2798–2832. doi:10.1021/ja01344a001.

[6] O. Michuta, P. Martuniuk, O. Ostapchuk, T. Tsvetkova. On non-isothermal soil water flow considering sorption effect, JP Journal of Heat and Mass Transfer, 18 (2019) 181–192. doi:10.17654/HM018010181

[7] J. Kärger, S. Brandani, C. Chmelik, D. V. Cortes, S. Fritzsche, H. Jobic, D. M. Ruthven, D. N. Theodorou. Diffusion in nanoporous materials with special consideration of the measurement of determining parameters, Pure and Applied Chemistry, 97 (2025) 1–89. doi:10.1515/pac-2023-1126.

[8] M. Petryk, J. Fraissard, S. Leclerc, D. Canet. Modeling of gas transport in a microporous solid using a slice selection procedure: Application to the diffusion of benzene in ZSM5, Catalysis Today, 139 (2008) 234–240. doi:10.1016/j.cattod.2008.05.034.

[9] S. Leclerc, M. Petryk, D. Canet, J. Fraissard. Competitive diffusion of gases in a zeolite using proton NMR and slice selection procedure, Catalysis Today, 187 (2012) 104–107. doi:10.1016/j.cattod.2011.09.007.

[10] M. Petryk, S. Leclerc, D. Canet, I. V. Sergienko, V. S. Deineka, J. Fraissard. Competitive diffusion of gases in a zeolite bed: NMR and slice selection procedure, modeling, and parameter identification, J. Phys. Chem. C, 119 (2015) 26519–26525. doi:10.1021/acs.jpcc.5b07974.

[11] I. V. Sergienko, M. R. Petryk, S. Leclerc, J. Fraissard. Highly efficient methods of the identification of competitive diffusion parameters in inhomogeneous media of nanoporous particles, Cybern. Syst. Anal., 51 (2015) 529–546. doi:10.1007/s10559-015-9744-7.

[12] M. Petryk, A. Doroshenko, D. Mykhalyk, P. Ivanenko, O. Yatsenko. Automated Parallelization of Software for Identifying Parameters of Intraparticle Diffusion and Adsorption in Heterogeneous Nanoporous Media. In: Mathematical Modeling and Simulation of Systems. MODS 2022. Lecture Notes in Networks and Systems, vol 667. Springer, Cham, 2023. doi:10.1007/978-3-031-30251-0_3.

[13] B. Mu, H. Liu. Prediction of the effective diffusion coefficient in random porous media using the finite element method, J. Porous Mater., 14 (2007) 63–70. doi:10.1007/s10934-006-9007-0.

[14] M. Petryk, A. Khimitch, M. M. Petryk. Simulation of adsorption and desorption of hydrocarbons in nanoporous catalysts of neutralization systems of exhaust gases using nonlinear Langmuir isotherm, Journal of Automation and Information Sciences, 50 (2018) 18–33. doi:10.1615/JAutomatInfScien.v50.i10.20.

[15] M. Petryk, A. Khimitch, M. M. Petryk, J. Fraissard. Experimental and computer simulation studies of dehydration on microporous adsorbent of natural gas used as motor fuel, Fuel, 239 (2019) 1324–1330. doi:10.1016/j.fuel.2018.10.134.

[16] L. Landau. To the theory of phase transitions. I, Z. Phys. Sowjetunion, 7 (1937) 19–32.

[17] A. P. Prudnikov, Yu. A. Brychkov, O. I. Marichev. Integrals and Series. Additional Chapters, Nauka, Moscow, 1986. 800 p.

[18] M. A. Lavrentiev, B. V. Shabat. Methods of the Theory of Functions of a Complex Variable, Nauka, Moscow, 1973. 736 p.

[19] A. Doroshenko, O. Yatsenko. Formal and Adaptive Methods for Automation of Parallel Programs Construction: Emerging Research and Opportunities. IGI Global, Hershey, Pennsylvania, USA, 2021. 279 p. doi: 10.4018/978-1-5225-9384-3.

[20] M. Rahbaralam, A. Abdollahi, D. Fernández-Garcia, X. Sanchez-Vila. Stochastic modeling of non-linear adsorption with Gaussian kernel density estimators, arXiv preprint arXiv:2004.06445 (2020). doi:10.48550/arXiv.2004.06445.

[21] E. A. Velikoivanenko, A. S. Milenin, A. V. Popov, V. A. Sidoruk, A. N. Khimich. Methods of numerical forecasting of serviceability of welded structures on computers of hybrid architecture, Cybernetics and Systems Analysis, 53 (2019) 117–127. doi:10.1007/s10559-019-0033-4.